2008 SCEC Annual Report
Frictional and thermal weakening during earthquake nucleation and the physics of fast versus slow slip

Paul Segall
Stanford University Geophysics Department

June 11, 2009

1 Introduction

Over the last few decades, the development of rate- and state-dependent friction has provided compelling models of earthquake nucleation. Concurrently, many researchers have considered thermal weakening mechanisms, including shear heating-induced thermal pressurization during rapid slip. The discovery of slow-slip events raises additional questions about processes that control the rate of localized fault slip. We have been exploring the mechanics of dilatant strengthening coupled to rate-state friction as a possible explanation for slow slip. In our 2008 proposal, we outlined a plan to study earthquake nucleation as it transitions from frictionally-dominated to thermal weakening-dominated, as well as the the role of dilatant strengthening in controlling whether nucleation becomes seismic or remains quasi-static.

With SCEC support, we have developed finite-difference codes that solve the coupled problems for 2D elastic, diffusive systems with a 1D fault. In the course of that research, we demonstrated that thermal pressurization typically becomes the dominant process during earthquake nucleation, well before seismic slip has occurred. We obtained the surprising result that thermal pressurization significantly reduces the length of the nucleation zone relative to that found with rate and state friction alone. For isothermal faults with dilatancy described by the *Segall & Rice* [1995] constitutive law, we showed that dilatancy can stabilize slip at rates well below inertial on velocity weakening faults. For a simplified "membrane diffusion" model we obtained a simple rule that predicts whether slip becomes dynamic or remains slow.

2 Governing equations

We model the slip zone in a greatly simplified manner by treating the principal shear zone as having zero width (that is, slip on a planar surface) Diffusion times across the low permeability fault core are much greater than earthquake nucleation times, so we treat the off-fault diffusive material as a homogeneous medium with low permeability. We also assume that diffusion of heat and pore pressure occurs only in the fault-normal direction. Slip on the fault is governed by rate- and state-dependent friction. For a detailed

explanation of the governing equations, see *Segall & Rice* [1995] and *Segall & Rice* [2006].

$$\text{Friction:} \quad \tau_{\text{fric}} = f\sigma_{\text{eff}} = \left[f_0 + a \ln \frac{v}{v_0} + b \ln \frac{\theta v_0}{d_c} \right] \sigma_{\text{eff}} \tag{1}$$

$$\text{“Aging” state evolution law:} \quad \frac{d\theta}{dt} = 1 - \frac{\theta v}{d_c} \tag{2}$$

$$\text{“Slip” state evolution law:} \quad \frac{d\theta}{dt} = -\frac{\theta v}{d_c} \ln \frac{\theta v}{d_c} \tag{3}$$

$$\text{Normal stress effect on state:} \quad \frac{d\theta}{dt} = \left[\begin{matrix} \text{state evolution} \\ \text{law (2) or (3)} \end{matrix} \right] - \frac{\alpha\theta}{b\sigma_{\text{eff}}} \frac{d\sigma_{\text{eff}}}{dt} \tag{4}$$

$$\text{Shear heating (zero-width shear zone):} \quad \left. \frac{\partial T}{\partial y} \right|_{y=0} = -\frac{\tau v}{2\rho c_v c_{\text{th}}} \tag{5}$$

$$\text{Dilatancy Constitutive Law:} \quad \frac{d\phi}{dt} = -\epsilon \frac{d}{dt} \ln \left(\frac{v_0 \theta}{d_c} \right) = -\frac{\epsilon}{\theta} \frac{d\theta}{dt}, \tag{6}$$

$$\text{Thermal pressurization (zero-width zone only):} \quad \Delta p(x{=}0) \; = \; \frac{\Lambda}{1 + \sqrt{c_{\text{hyd}}/c_{\text{th}}}} \Delta T(x{=}0) \tag{7}$$

$$\text{Thermal pressurization factor:} \quad \Lambda = \frac{\lambda_f - \lambda_\phi}{\beta_f + \beta_\phi} \tag{8}$$

$$\text{Isothermal Membrane Diffusion:} \quad \frac{\partial p}{\partial t} = \frac{p^\infty - p}{t_f} - \frac{1}{\beta} \frac{\partial \phi}{\partial t} \tag{9}$$

For thermal pressurization calculations without dilatancy, equation (5) becomes a boundary condition on a homogeneous diffusion equation for temperature with thermal diffusivity c_{th} (e.g. *Rice* [2006]). For uniform transport properties *Rice* [2006] showed that there is a unique relationship between temperature on the fault and pore-pressure on the fault (7). This is combined with the frictional consitutive equations and two dimensional elasticity equations to yield a consistent set of governing equations. In another set of numerical experiments we ignore thermal effects and consider the influence of dilatancy with the simplified “membrane diffusion” transport model (9), where t_f is a characteristic diffusion time. In these equations α is the Linker-Dieterich constant, ρ is density, c_v is heat capacity, ϕ is porosity, λ's are thermal expansivities, and β's are compressibilities; subscripts $_f$ indicate pore-fluid, and $_\phi$ indicate pores.

3 Results

A consistent result from our work modeling thermal pressurization without dilatancy is that it has the effect of preventing growth of the nucleation zone. Figure (1) shows a comparison of isothermal, drained (that is, “regular”) nucleation to nucleation with thermal pressurization for the aging law form of the state evolution equations. Results for isothermal simulations alongside results for simulations with thermal pressurization are shown in Fig. 1. The first plot shows snapshots of slip speed for the isothermal case. The result is similar to those of *Ampuero & Rubin* [2008] in that the nucleation zone takes the form of a quasi-statically growing crack—slip speed is roughly constant inside the growing nucleation zone. With thermal pressurization (second plot), however, such a slip speed profile never occurs. At the moment when the crack-like form should arise (about when $v_{\max} \approx 10^{-5}$ m/s), slip continues to accelerate at the center of the nucleation zone, and fast slip eventually concentrates there.

The visual difference in the character of the slip speed profiles in Fig. 1 hints at a “critical velocity” v_{crit} that defines the speed at which thermal pressurization dominates fault strength. We quantify v_{crit} from our simulations by comparing the magnitude of the two terms in the frictional weakening equation $d\tau_{\text{fric}}/dt = [(\sigma - p_0)d\mu/dt] - [f_0 dp/dt]$, which are respectively the frictional term and the thermal pressurization term. Figure 2 shows graphically the determination of v_{crit}. For nominal values of friction parameters

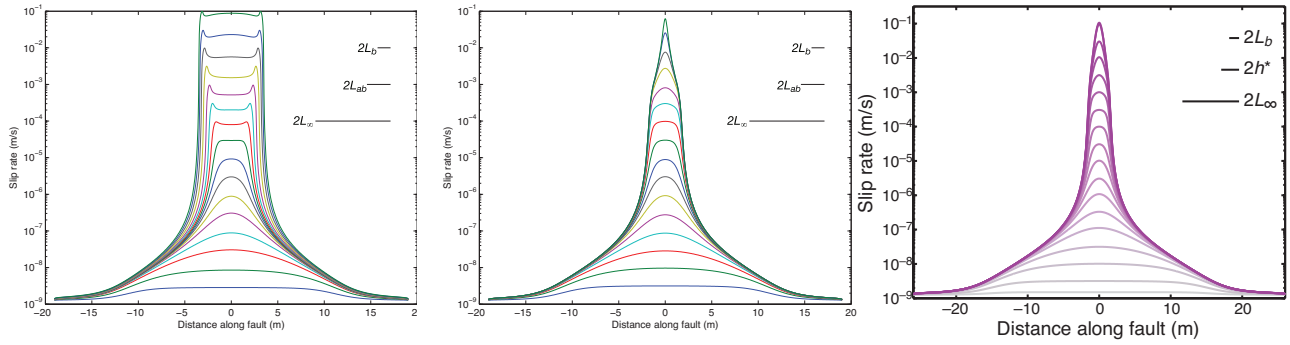

Figure 1: Results from aging law simulations in the isothermal (left) and thermal pressurization (right) cases. In these simulations, $a/b = 0.8$, $d_c = 100$ μm, $\alpha = f_0 = 0.6$, and $(\sigma - p_0) = 140$ MPa. Lines represent snapshots taken at times corresponding to half-decade increases in maximum slip speed $v_{\max}$ from $10^{-9.5}$ m/s to 10^{-1} m/s. **(a)** Snapshots of slip speed for isothermal, drained, aging-law nucleation. Scale bars show L_b [*Dieterich*, 1992], $L_{ab} = Gd_c/(b-a)\sigma_{\text{eff}}$, and L_∞ [*Ampuero & Rubin*, 2008]. **(b)** Snapshots of slip speed with thermal pressurization. Comparing to (a), note that at early times (low slip speeds) the profiles are similar to the isothermal simulation. At $\sim 10^{-5}$ m/s, the profiles start to diverge. By $\sim 10^{-4}$ m/s, the profiles have distinctly different forms. The sharp peak at higher slip speeds indicates how slip is evolving toward a singularity of high slip over a zero-width area. **(c)** Snapshots of slip speed with thermal pressurization and the *Linker & Dieterich* [1992] effect with $\alpha = f_0 = 0.6$. The inclusion of this effect prevents the development of a slip singularity.

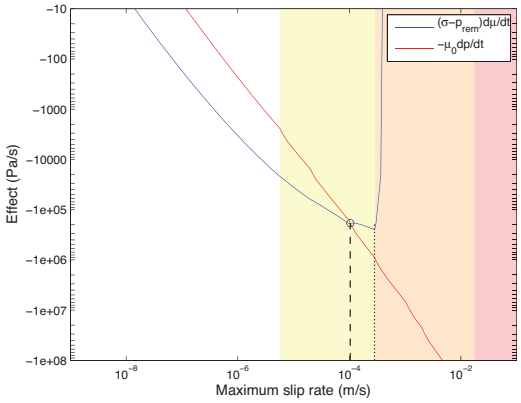

Figure 2: Weakening rates at the fastest-slipping point in the fault for time-dependent friction and pore pressure, as decomposed in the text. Critical velocity v_{crit} is shown with vertical dashed lines and is defined when $-f_0 dp/dt > (\sigma - p_0)d\mu/dt$. The shaded regions indicate the validity of the planar shear zone approximation. Yellow signifies $\Delta y \leq 100h$, orange signifies $\Delta y \leq 10h$, and red signifies $\Delta y \leq h$. The planar shear zone assumption used here is valid only for $\Delta y \gg h$, and a reasonable estimate is $h \approx 100$ μm.

and effective stress, v_{crit} is on the order of 0.1 to 1 mm/s, indicating that thermal weakening dominates rate-state weakening late in the nucleation process, well before seismic radiation effects are important.

We find that with standard rate-state friction and thermal pressurization, the concentration of slip at the center of the nucleation zone leads to a singularity in slip speed; the middle plot of Fig. 1 shows the nucleation zone concentrating toward a point. Following a suggestion of Jim Dieterich we included the effect of variable normal stress on frictional state, identified in *Linker & Dieterich* [1992]. There, the authors conducted experiments in which rock samples were slid at constant velocity while step changes in normal stress were applied. Shear stress did not immediately take on its new value; rather, it evolved toward a value appropriate to the newly imposed normal stress over a characteristic slip distance d_c, which follows equation (4) above. This effect is relevant to the thermal pressurization problem because fault weakening occurs via decreasing effective normal stress $\sigma_{\text{eff}} = \sigma - p(t)$. The third plot in Fig. 1 shows the effect of the *Linker & Dieterich* [1992] mechanism. In that case, we use $\alpha = f_0$, which completely regularizes the problem and prevents the development of a slip singularity. This result indicates that it is important to include the *Linker & Dietrich* [1992] effect when dynamic weakening mechanisms influence σ_{eff}.

All of our work thus far has made use of the planar shear zone approximation, which is valid for times that are much greater than the diffusion time across a real shear zone width h. At high slip speeds, however, this approximation is no longer valid. As discussed in the caption to Fig. 2, the planar shear zone approximation is not valid at speeds greater than roughly $v_{\rm crit}$. At such speeds, the heat production is sufficiently large that the simulations must take small time steps to maintain accuracy, and these time steps are no longer much greater than a realistic diffusion time across a shear zone. The color coding in Figure 2 attempts to qualitatively evaluate the validity of the planar shear zone approximation. In 2008, we began work on implementing a finite-width shear zone to address this issue; that work is ongoing. In a finite shear zone, we expect the thermal pressurization effect to be somewhat diminished because the heat sources are distributed, which would cause the peak pressurization on the fault to be lower. This effect should also act to regularize the non-physical contraction of the nucleation zone, as exhibited in Fig. 1b.

Our work on thermal pressurization during nucleation continues. We are currently completing our study of thermal pressurization in the zero-width shear zone. We have been exploring the thermal pressurization effect in the context of slip-law nucleation. Preliminary results suggest that it is similar to aging-law nucleation for frictional parameters $a/b < 0.8$, which is surprising because it indicates that thermal pressurization may in that case prevent the pulse-like nucleation zone associated with the slip law. For a/b near 1, the pulse-like nucleation zone arises at speeds much lower than our $v_{\rm crit}$, and we are currently examining those cases.

We have demonstrated that, at least for nucleation the aging law, thermal pressurization strongly restricts the growth of the nucleation zone. A major consequence is that it will be extremely challenging to detect precursory strain associated with a developing nucleation zone, which was a possibility mentioned by *Ampuero & Rubin* [2008] for aging law nucleation with a/b near 1. While the immediate prospect of application of this work to earthquake hazard mitigation is somewhat discouraging, this work will be of use to researchers who model dynamic rupture, since it will give insight into the initial heat and pore fluid conditions of their models.

We have also continued exploring the potential for dilatancy to stabilize instability, leading to slow slip events on nominally velocity weakening faults. An appealing feature of this model is that the faster the fault slips the more difficult it is for pore-fluid flow into the fault to keep up, hence the fault zone pore-pressure decreases, increasing the effective normal stress and stabilizing slip. Early work has focused on the isothermal "membrane diffusion" transport model (9). The width of the fault for which friction and dilatancy are computed is W. Outside this region constant slip-rate equal to the plate velocity v^∞ is imposed on both edges (symmetric loading), or on one side with the other side set to $10^{-3}v^\infty$ (asymmetric loading), to roughly approximate a frictionally locked interface. For this model there are two important non-dimensional parameters, other than the friction ratio a/b that control the system dynamics. The first,

$$\mathcal{E} \equiv \frac{f_0 \epsilon}{\beta b(\sigma - p^\infty)} \tag{10}$$

gives the importance of dilatancy relative to frictional weakening. This scaling arises because dilatant strengthening scales with $f_0\epsilon/\beta$, whereas the frictional weakening scales with $b(\sigma - p^\infty)$. Note that dilatancy is relatively stronger when the effective stress is low. The fluid transport term in (9) depends on

$$\mathcal{U} \equiv \frac{v^\infty t_f}{d_c} \tag{11}$$

the ratio of the characteristic fluid diffusion time to the characteristic time for state evolution. When $\mathcal{U} \gg 1$ the system is effectively undrained, whereas when $\mathcal{U} \ll 1$ the fault is drained.

Figure 3 shows a sample calculation with the slip law form of the evolution equation and $\mathcal{E} = 1, a/b = 0.833, W/h^* = 8$, where h^* is the drained critical dimension for nucleation. Slip propagates from the right to left driven by the increasing displacement at the right boundary. The maximum slip-rate increases as the

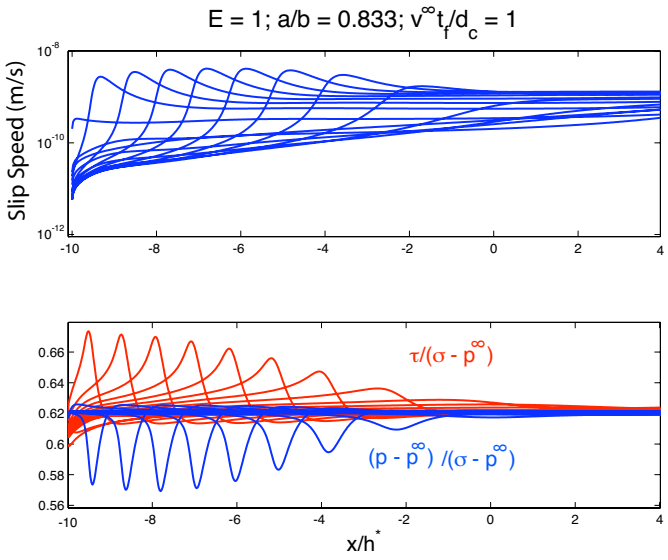

Figure 3: A representative calculation with asymmetric loading. Each curve represents a snapshot in time. Slip event propagates from right to left. top) slip speed. bottom) shear stress and pore pressure change, both normalized by nominal effective stress. Isothermal, membrane diffusion approximation.

crack grows, but remains less than an order of magnitude above v^∞. In these calculations v^∞ is taken to be 0.04 m/yr $= 1.3 \times 10^{-9}$ m/s. Figure 3 also shows a significant stress concentration as well as pore-pressure reduction at the front of the propagating crack. It is the relative suction at the crack tip that stabilizes the slip against dynamic instability. Note that without dilatancy this solution, with $W/h^* = 8$ and the slip law, would reach inertially limited slip rates. However, with membrane diffusion, and the specified material parameters, slip is stable for $W/h^* \leq 40$ (we have tested cases to at least 90), whereas without dilatancy slip becomes dynamic for $W/h^* \sim 3$.

A linearized stability analysis based on the approach of *Segall & Rice* [1995] leads to the conclusion that dilatancy will stabilize slip over a very broad range of W/h^* if $\mathcal{E}$ exceeds a critical value given by

$$\mathcal{E}_{crit} \geq 1 - \frac{a}{b}. \tag{12}$$

Numerical analyses were conducted for different values of a/b and $\mathcal{E}$, recording the maximum slip rates achieved in each simulation. Maximum slip speeds were recorded many cycles after the onset of the calculation to ensure that the values are not strongly dependent on the initial conditions. Results are shown in Figure 4. If the maximum slip speed reaches dynamic values (taken to be 0.1 m/s) for a sufficiently large weakening zone W/h^* (a wide range around the predicted critical value is tested) the result is indicated in red. If, however, the behavior is quasi-static regardless of W/h^* the result is indicated in black. The line $\mathcal{E} = 1 - a/b$ does a remarkably good job of dividing the space into fast and slow slip behavior. The numerically inferred boundary lies slightly below the line $\mathcal{E} = 1 - a/b$, at least for large a/b where the friction alone is nearly velocity neutral.

The result in Figure 4 indicates that we have a reasonable understanding of the dilatancy stabilization for the isothermal membrane diffusion model. Current work is focusing on first including a more realistic homogeneous pore-fluid diffusion model. This is done with by coupling a finite difference diffusion calculation to the friction-elasticity equations as in the thermal pressurization work. Preliminary results from these calculations are qualitatively similar to the membrane diffusion model. Upcoming work will be to couple the thermal pressurization and dilatancy effects. This will allow us to test the overarching hypothesis

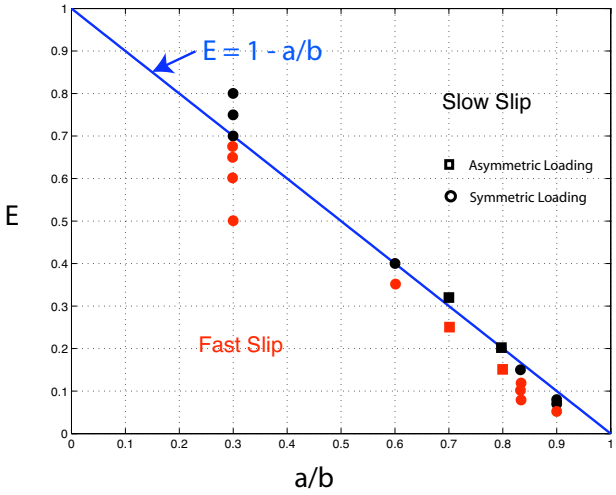

Figure 4: Stability boundary between fast and slow slip. Each symbol may represent multiple runs with varying W/h^*. Red symbols indicate solutions that reach radiation damping velocities for a sufficiently large W/h^*. Black symbols represent solutions that never reach inertially limited slip speeds regardless of W/h^*. Square symbols are loaded from one side, circles are loaded from both sides. Line $\mathcal{E} = 1 - a/b$ is the linearized stability boundary between stable and unstable domains.

that whether slip becomes inertially limited (fast earthquake) or remains slow, depends on the competition between diltatant strengthening and thermal weakening.

References

[1] Ampuero, J.-P. and A. M. Rubin (2008), Earthquake nucleation on rate and state faults—Aging and slip laws, *J. Geophys. Res., 113*, B01302, doi:10.1029/2007JB005082.

[2] Dieterich, J. H. (1992), Earthquake nucleation on faults with rate- and state-dependent strength, *Tectonophysics, 211*, 115–134.

[3] Linker, M. F. and J. H. Dieterich (1992), Effects of variable normal stress on rock friction: Observations and constitutive equations, *J. Geophys. Res., 97*(B4), 4923–4940.

[4] Liu, Y., and J. R. Rice (2007), Spontaneous and triggered aseismic deformation transients in a subduction fault model, *J. Geophys. Res., 112*, B09404, doi:10.1029/2007JB004930.

[5] Rice, J.R., Heating and weakening of faults during earthquake slip, *J. Geophys. Res., 111*, B5, doi:10.1029/2005JB004006, 2006.

[6] Segall, P. and J. R. Rice (1995), Dilatancy, compaction, and slip instability of a fluid saturated fault, *J. Geophys. Res., 100*, 22,155-22,171.

[7] Segall, P. and J. R. Rice (2006), Does shear heating of pore fluid contribute to earthquake nucleation?, *J. Geophys. Res., 111*, B09316, doi:10.1029/2005JB004129.